GL01144

IDO/77.5.7
Distribution Category UU-66a
ESL-4

LOW-ALTITUDE AEROMAGNETIC SURVEY OF A PORTION OF THE COSO HOT SPRINGS KGRA, INYO COUNTY, CALIFORNIA

Richard C. Fox

May, 1978

Work performed under Contract No. EY-76-S-07-1601

NOTICE

This report was prepared to document work sponsored by the United States Government. Neither the United States nor its agent, the United States Department of Energy, nor any Federal employees, nor any of their contractors, subcontractors or their employees, makes any warranty, express or implied, or assumes any legal liability or responsibility for the accuracy, completeness, or usefulness of any information, apparatus, product or process disclosed, or represents that its use would not infringe privately owned rights.

NOTICE

Reference to a company or product name does not imply approval or recommendation of the product by the University of Utah Research Institute or the U.S. Department of Energy to the exclusion of others that may be suitable.

IDO/77.5.7
Distribution Category UU-66a
ESL-4

LOW-ALTITUDE AEROMAGNETIC SURVEY OF A PORTION OF THE COSO HOT SPRINGS KGRA, INYO COUNTY, CALIFORNIA

Richard C. Fox

EARTH SCIENCE LABORATORY
UNIVERSITY OF UTAH RESEARCH INSTITUTE
391-A Chipeta Way
Salt Lake City, Utah 84108

Date Published - May 1978

Prepared for the
DEPARTMENT OF ENERGY
DIVISION OF GEOTHERMAL ENERGY
UNDER CONTRACT EY-76-S-07-1601

TABLE OF CONTENTS

LIST OF ILLUSTRATIONS

ABSTRACT

A detailed low-altitude aeromagnetic survey of 576 line-mi (927 line-km) was completed over a portion of the Coso Hot Springs KGRA in September 1977. The survey has defined a pronounced magnetic low that could help delineate the geothermal system. The magnetic low has an areal extent of approximately 10 sq mi (26 sq km). Direct and indirect evidence indicates that this anomaly is due, in part, to magnetite destruction by hydrothermal solutions associated with the geothermal system. The anomaly generally coincides with two other geophysical anomalies which are directly associated with the system: 1) a bedrock electrical resistivity low, and 2) an area of relatively high near-surface temperatures. The highest measured heat flow, 18 HFU, also occurs within its boundary.

The magnetic low occurs at the intersection of two major structural zones which coincide with a complementary set of strike-slip fault zones determined from seismic activity. The intersection of these two zones of active tectonism probably served as the locus for emplacement of a pluton at depth, above which are observed the coincidental geophysical anomalies and surface manifestations related to the geothermal system.

INTRODUCTION

On behalf of the U.S. Department of Energy, Division of Geothermal Energy, geological and geophysical studies were conducted for a portion of the Coso Hot Springs KGRA (Fig. 1) by the Earth Science Laboratory, University of Utah Research Institute. These studies served two purposes: 1) evaluation and interpretation of results from the drilling and logging of CGEH-1 (Galbraith, 1978), and 2) determination of possible sites for future drill tests. Investigations for the latter were carried out during September and October, 1977 and included geologic and alteration mapping (Hulen, 1978), a detailed electrical resistivity survey (Fox, 1978) and a low-altitude aeromagnetic survey, the results of which are the subject of this report.

A regional aeromagnetic survey of the Coso area was completed in 1975 by the U.S. Geological Survey (Open-file report 76-698) which covered an area 32 mi E-W by 30 mi N-S (51 by 48 km) centered approximately on Coso Hot Springs. The survey altitude was 7000 feet (2135 m) above sea level, approximately 2500 feet (762 m) above the mean terrain elevation of the present survey area, and the flight line spacing was one mile (1.6 km). These survey characteristics precluded the recording of local, small scale changes in magnetization.

The present survey was flown to generate a detailed magnetic map that could show local variations in rock magnetization and magnetic features related to structures that would help delineate the geothermal system.

GEOLOGY

The Coso Range, in which the Coso KGRA is located, occurs in the western Basin and Range province. It was formed primarily by dip-slip movement along


CALIFORNIA
0 20 40 60 80
MILES
N
LOCATION MAP
COSO HOT SPRINGS
KGRA
OREGON
DEL NORTE
Crescent City
Yreka
MODOC
Alturas
SISKIYOU
HUMBOLDT
Eureka
TRINITY
SHASTA
LASSEN
Weaverville
Redding
Susanville
Red Bluff
TEHAMA
PLUMAS
Quincy
MENDOCINO
GLENN
BUTTE
Willows
Oroville
SIERRA
Downieville
COLUSA
NEVADA
Ukiah
Lake-port
Colusa
Yuba City
YUBA
Nevada City
Marysville
PLACER
Auburn
LAKE
YOLO
SUTTER
EL DORADO
SONOMA
Placerville
Markleeville
NAPA
Wood-land
Sacramento
Santa Rosa
SACRA-MENTO
AMADOR
Jackson
ALPINE
Napa
Fair-field
CALAVERAS
Bridgeport
MARIN
SOLANO
SAN JOAQUIN
San Andreas
TUOLUMNE
San Rafael
Martinez
Sonora
CONTRA COSTA
Stockton
San Francisco
SAN FRANCISCO
Oakland
Modesto
MONO
ALAMEDA
MARIPOSA
Redwood City
SAN MATEO
San Jose
STANISLAUS
Mariposa
SANTA CLARA
Merced
MADERA
SANTA CRUZ
Santa Cruz
MERCED
Madera
FRESNO
Hollister
Salinas
SAN BENITO
Fresno
Independence
Hanford
Visalia
INYO
MONTEREY
KINGS
TULARE
SAN LUIS OBISPO
Bakersfield
San Luis Obispo
KERN
SAN BERNADINO
SANTA BARBARA
VENTURA
LOS ANGELES
Santa Barbara
Ventura
San Bernardino
Los Angeles
Riverside
Santa Ana
RIVERSIDE
ORANGE
ARIZ.
SAN DIEGO
IMPERIAL
San Diego
El Centro
MEXICO

FIGURE 1

northerly-trending, high-angle normal faults. Within the survey area, the Basin and Range structure is disrupted by west-northwest, northwest and north-trending high-angle faults. Plate I covers the survey area and a corresponding portion of the Coso Range as mapped by Duffield and Bacon (1977). This map shows the surface geology as a Late Cenozoic basaltic to rhyolitic volcanic sequence resting on a Mesozoic (?) basement complex.

The volcanic sequence includes several prominent rhyolitic domes and a lesser number of basaltic domes. Although the basement complex is not subdivided on this map, Duffield and Bacon (1977, sheet 2) indicate that it consists principally of granitic intrusive rock and ranges in composition from granite through quartz-diorite to diorite or gabbro. Hulen (1978) in an accompanying report states that the granitic intrusives, Jurassic-Late Cretaceous in age, are probably satellites of the southern Sierra Nevada Batholith.

AEROMAGNETIC SURVEY

The total-field aeromagnetic survey was conducted by Aerial Surveys of Salt Lake City, Utah. The survey flown in September, 1977 covers an area extending 12 mi N-S by 12 mi (19 km sq) E-W, centered on Devil's Kitchen. The flight altitude was 750 feet (229 m) above mean terrain with a one-quarter mile (403 m) line spacing. A total of 576 line-mi (927 line-km) was surveyed. Data were recorded in analog format and digitally on magnetic tape. The terrain clearance along the flight line was maintained by digital readout from a radar altimeter during the survey and was continuously recorded in analog form on a strip chart recorder. A continuously recording ground magnetic

station recorded diurnal changes in the magnetic field and monitored magnetic storm activity. Topographic base maps for the surveyed area include the USGS 15 minute topographic series quadrangles of Haiwee Reservoir, Coso Peak, Little Lake and Mountain Springs Canyon.

The survey results were compiled manually. A flight line map was made by matching images on 35 mm strip film of the flight lines to images on aerial photographs (scale 1:18,000) of the surveyed area taken at the start of the survey. Intermediate points along each flight line were located by linear interpolation between the recovered points. The flight lines located on the aerial photo base were rectified to an accurate topographic base by transforming points from the photo base to corresponding points on a 1:18,000 scale topographic map. Magnetic values for fiducial numbers corresponding with the recovered points and maximum and minimum magnetic values observed between recovered points were taken from the analog records and posted along the flight lines. The final map was compiled at a scale of 1:24,000 with a 25 gamma contour interval. A base level value of 50,000 gammas was subtracted from the observed total field values.

INTERPRETATION

Magnetic Anomalies

The sources of several magnetic anomalies were identified by correlating the magnetic anomalies, Plate II, with the topography and geology, Plate I. These anomalies are identified by reference points (RP) on Plate III. The source outlines shown on this plate are only approximate outlines of the actual magnetic sources and are shown mainly for the purpose of locating the

source areas. Table I shows the probable source rock type, and probable causes of the anomalies. Except for RP-17, all of the identified anomalies have sources that are attributable to the outcropping rock in their source areas.

TABLE I

Interpretation of Magnetic Anomaly Sources

Reference Point	Probable Rock Type	Probable Cause
RP - 1, 2, 3, 17	Diorite or Gabbro	SC*
RP - 4, 6, 7, 8, 9, 10, 11, 13, 14, 15, 18, 19, 20, 25, 29, 30, 31	Rhyolite	SC+TE*+RM*
RP - 5, 23, 26, 27, 28 40	Basalt	SC+TE+RM
RP - 12	Dacite	SC+TE+RM
RP - 16, 22, 34, 35	Basalt	SC+RM
RP - 21	Granite(?)	SC+TE
RP - 24	Andesite	SC+TE+RM
RP - 32, 33, 36, 37, 38, 39	Quartz-diorite(?)	TE

*SC = Susceptibility Contrast
*TE = Terrain Effect
*RM = Remanent Magnetization

Many of these anomalies show a strong correlation with topography, e.g., the rhyolite domes. Topographic-effect magnetic anomalies are caused by magnetic terrain features. Variations in terrain clearance between the airborne magnetometer and the topographic surface can significantly contribute to the observed anomalies, especially in a low altitude survey like this. Both magnetic highs and lows can be generated by topographic features as shown by Figure 2.

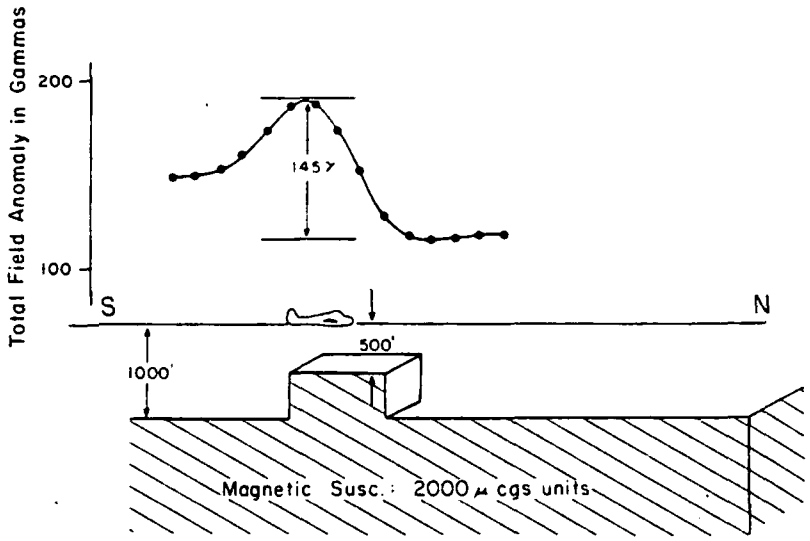

Topo Feature

width	length	height
1000'	1000'	500'

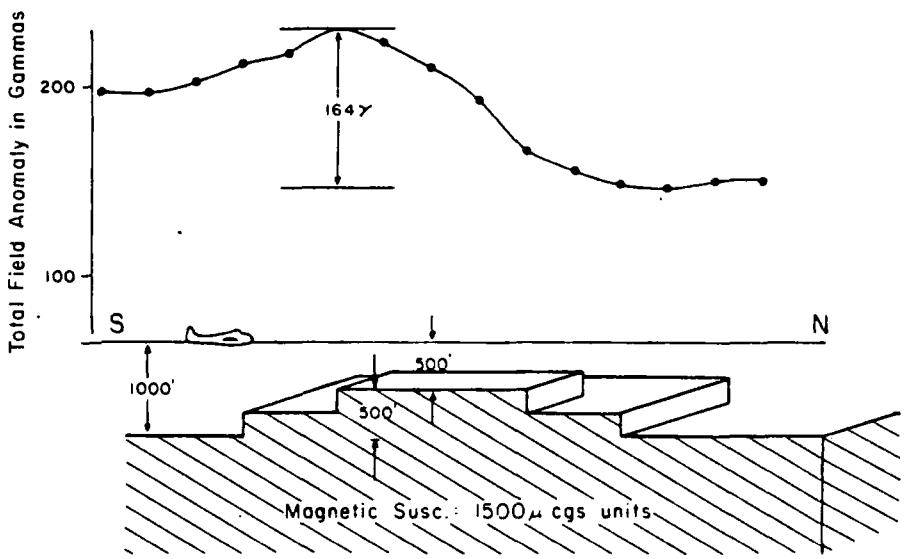

Topo Feature

width	length	height
4000'	4000'	250'
2000'	2000'	250'

Total Relief 500'

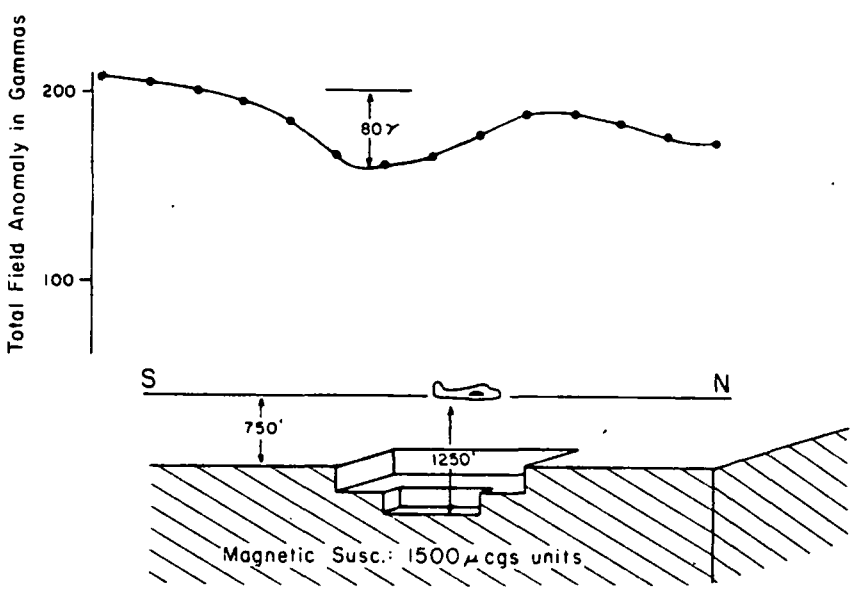

Topo Feature

width	length	depth
2000'	2000'	250'
1000'	1000'	250'

Total Relief 500'

FIGURE 2

TOPOGRAPHIC EFFECT MAGNETIC ANOMALIES

Earth's Magnetic Field Strength: 50,000 gammas

Declination = 16° E; Inclination = 60°

Preliminary attempts to determine the magnetization and source geometry for the rhyolite domes indicated some degree of remanent magnetization contributed to their observed anomalies. Various domes were individually modelled using vertical-sided, right-regular prisms with 10,000 ft (3050 m) of depth extent. The area of the models, in plan view, approximated the outcrop area of the individual domes as shown on Plate I. The apparent magnetic susceptibilities assigned to these models to match the observed anomalies are in the range 1000-2000 micro-cgs units. To make the geometry of these simple models conform more closely to a reasonable geometry for the root systems of the domes, e.g. an inverted cone or funnel, would cause an attendant volume decrease which would have to be offset by an increase in apparent magnetic susceptibility. Apparent susceptibilities larger than 2000 micro-cgs are unusual for rhyolites in general and could be explained by a remanent magnetization component. The magnetic susceptibility of a rock, k, is the ratio of the intensity of its induced magnetic anomaly, I, to the intensity of the inducing magnetic field, H, that is $k = \frac{I}{H}$. If a rock is permanently magnetized in a direction that adds to the magnetic anomaly due only to induction by the earth's magnetic field, it will have an interpreted or apparent susceptibility that is higher than the true susceptibility expected for the given rock type.

A common feature of most of the rhyolite domes is a positive magnetic expression. Variations in the amplitudes of their anomalies are due to several factors such as variations in: 1) magnetic susceptibility of the domes or between the domes and their host rock, 2) remanent magnetization, 3) terrain clearance, or 4) flight line location. None of these factors readily

explain the lack of magnetic expression of the dome at RP-15a (Plate III). Either this dome has no appreciable root system (volume of magnetic material) or, if it does, the magnetite within its root structure has been altered by hydrothermal solutions to non-magnetic hematite or pyrite. If the latter explanation is the actual case, the age determined for this dome of less than 100,000 years (Lanphere and Dalrymple, 1975) suggests that the magnetite alteration could be caused by hydrothermal fluids associated with the present geothermal system.

Basement Magnetization

Broad west-northwest trending zones of contrasting magnetic intensity have been delineated on Plate III that define the gross magnetic characteristics of the area. The intensity levels assigned to each zone are taken from the contoured magnetic values shown on Plate II. These are residual total magnetic field values after a base level of 50,000 gammas was subtracted from the observed values. The two zones of low magnetic intensity, generally less than 1000 gammas, are interpreted to be caused by granitic basement rock. The zones of intermediate magnetic intensity, 1000 to 1200 gammas, are attributed to quartz-diorite and the high magnetic intensity zones, greater than 1200 gammas, to the diorite or gabbro end of the basement composition range. The margins of these zones are gradational between intermediate and high intensity zones but sharp between low and intermediate and between low and high zones. The sharp gradients are, in part, coincidental with west-northwest, trending mapped faults (Plate I) and thus may represent structural boundaries between adjacent zones. The sharp boundary between the southernmost low magnetic intensity zone and the adjacent

intermediate zone may be the northern edge of the west-northwest trending Wilson Canyon fault system which projects through this area (Furgerson, 1975, pg. 2). The sharp boundary between the zone of low magnetic intensity associated with the Haiwee trend and the zone of high magnetic intensity to the south may reflect the southern edge of the Haiwee fault system.

A magnetic profile that crosses the three levels of magnetic intensity (see Plate III for location) was analyzed to determine the range of apparent magnetic susceptibilities that are associated with these levels. Figure 3 shows the observed and computed magnetic gradient and the model used to make the analysis. As constructed, the model takes into account the variation in terrain clearance along the profile as observed on the terrain clearance analog record for this profile. Each prism of the model extends 10,000 feet (3500 m) to the east and to the west of the profile to approximate the general east-west linear trend in terrain elevation (Plate I) and to produce the observed east-west linear trend in magnetic intensity (Plate II). The prisms extend to 10,000 feet below the line of observation. This depth extent was chosen to insure that the computed magnetic gradient would be only a function of the topographic relief and the horizontal change in magnetic susceptibility and would not be influenced by the depth extent of the prisms. Figure 3 shows that an increase in magnetic susceptibility of 3000 micro cgs units across the zones from low to high magnetic intensity is required to generate the observed gradient.

Magnetic susceptibilities were measured on ten foot (3 m) samples of drill cuttings from 430 intervals of drill hole CGEH-1. The samples were

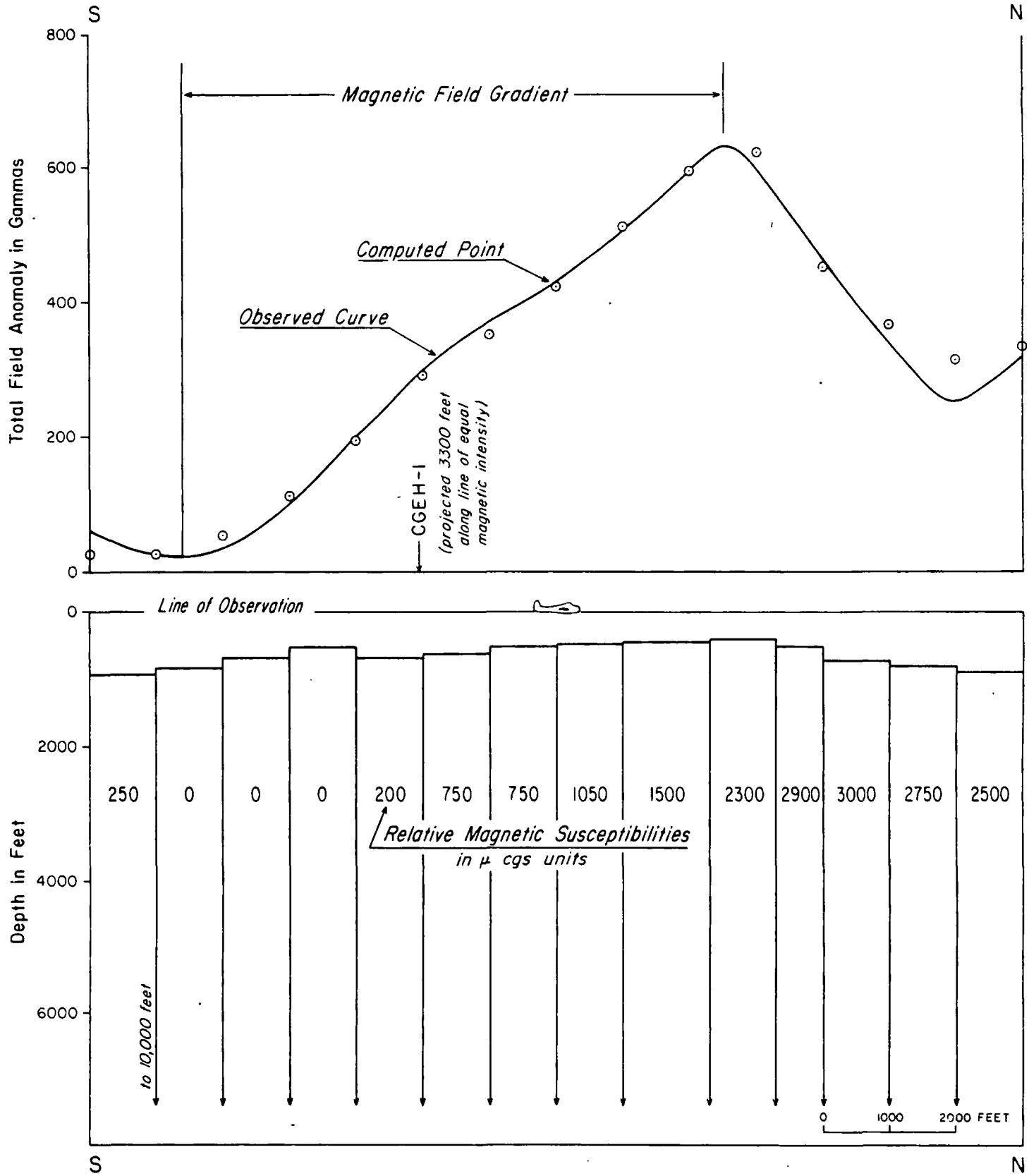

FIGURE 3

ANALYSIS OF MAGNETIC FIELD GRADIENT

(see Plate 3 for location of profile)

placed into four general categories according to composition (Galbraith, 1978), that are consistent with those used by Hulen (1978) to group the surface rocks he observed within this area. These categories are: 1) an older, pre-Late Cretaceous intermediate-to-mafic metamorphic sequence, 2) post-metamorphic quartz-latite porphyry and felsite, 3) Late Cretaceous (?) granite and allied intrusives (leucogranite and alaskite) and 4) Late Cenozoic volcanics (rhyolite). Based upon thin-section analysis, these rock types encountered in CGEH-1 appear only slightly altered (Galbraith, 1978). The majority of samples fall in either the metamorphic or granite and allied intrusive categories. The average magnetic susceptibility value for 154 samples in the metamorphic category is 1118 micro cgs units with a standard deviation of 849 micro cgs; that for 143 samples in the granite and allied intrusive category is 547 micro cgs units with a deviation of 566 micro cgs. Because of the weak susceptibility contrast (about 500 micro cgs) documented in the cuttings the observed magnetic gradient cannot be caused by a gradational horizontal change between the two major rock types observed in CGEH-1. These rock types are representative of the surface rocks in the area of the observed gradient. Assigning the metamorphic sequence with its average measured susceptibility (1118) to the zone at the high magnetic intensity end of the observed gradient and the granitic intrusives with their average susceptibility (547) to the low end will not give the computed change (3000) in susceptibility required to produce the observed gradient. Factors that could account for this apparent discrepancy are: 1) an increase in mafic content of the metamorphics within the high intensity zone giving an attendant increase in magnetic susceptibility, and 2) an attendant decrease in the

original or primary magnetite content of the granitic intrusives within the low intensity zone or the destruction of magnetite in the granitic intrusives as a result of hydrothermal alteration. Some combination of these factors is most likely. Measurements of the magnetic susceptibility of outcrop samples along the line of profile, Plate III, are required to determine to what degree each of these factors contribute to the observed gradient. If it can be shown that magnetite destruction is a significant factor, this would have an important bearing on the interpretation of the magnetic low outlined on Plate III.

Structure

Based on analyses of seismic activity, Weaver and Walter (1977) describe a northwest trend of right-lateral, strike-slip faulting, the Haiwee trend, and a complimentary northeast trend of left-lateral, strike-slip faulting, the Red Hill trend. These geographic names are given to the two structural zones shown on Plate III since their southwestern and northwestern portions conincide, respectively, to the Red Hill and the Haiwee trends described by Weaver and Walter. Plate III shows the Haiwee trend corresponds to a zone of low magnetic intensity and several similarly trending faults shown on Plate I. The Red Hill trend is well defined on the magnetic map from Sugarloaf Mountain to the southwest. The major east-northeast fault mapped by Hulen (1978), Plate III, is evidence for a continuation of this trend to the northeast through Devil's Kitchen and Coso Hot Springs. The trace of this fault is delineated by the canyon through the eastern side of the Coso Range between Devil's Kitchen and Coso Hot Springs. The fault is quite important since the fumerolic activity is either on or along the projection of its trace. The

deeply-incised, northeast-trending canyons through the basalt flows east of Coso Hot Springs may be fault-related and as such could represent a continuation of the Red Hill structural zone. The USGS aeromagnetic map and geologic map show east-northeast magnetic trends, topographic lineations and inferred faults that support the interpretation of a through-going, east-northeast structural zone. The structural zones shown on Plate III could help define zones of active tectonism by association with the zones of active seismicity.

Magnetic Low

The magnetic low outlined on Plate III is the most significant feature delineated by this survey with respect to the Coso geothermal system. It generally coincides with two other geophysical anomalies obviously related to the geothermal system, a bedrock electrical resistivity low (Fox, 1978) and an area of high, near-surface temperatures defined by LeSchack (1977). The highest measured rate of heat flow, 18 HFU (Combs, 1975), and evidence for hydrothermal bedrock alteration and magnetite destruction, mapped by Hulen (1978), both occur within its boundary. This direct evidence of magnetite destruction (although not pervasive), the lack of magnetic expression of the rhyolite dome at RP-15a, and the analysis of the magnetic field gradient (Figure 3), give reason to think that the magnetic low is partially due to magnetite destruction which is directly related to hydrothermal fluids within the geothermal system. The southern one-half of the low is due, in part, to an induced polarization low associated with the zone of high magnetic intensity at the southern boundary of the low. A polarization low is induced by the earth's magnetic field at the northern boundary of a magnetic source

with higher magnetic susceptiblility than its host rock.

Comparison of High- and Low-Altitude Magnetic Maps

Plate VI shows a portion of the USGS, 7000 foot (2135 m) constant-barometric-altitude, aeromagnetic map that corresponds with the low altitude survey. This map shows what can be considered to be an 'upward continuation' of the observed low-altitude magnetic field (Plate III). Local anomalies over volcanic domes and those resulting from terrain effects are completely attenuated while the west-northwest trending zones of contrasting magnetic intensity, Plate III, the two complimentary structural trends and the associated magnetic low are still readily apparent.

SUMMARY AND CONCLUSIONS

A low-altitude aeromagnetic survey of a portion of the Coso Hot Springs KGRA has defined a pronounced magnetic low that could help delineate the geothermal system. The magnetic low has an areal extent of approximately 10 sq mi (26 sq km). Direct and indirect evidence indicates that this anomaly is due, in part, to magnetite destruction by hydrothermal solutions associated with the geothermal system. It is significant that this anomaly generally coincides with two other geophysical anomalies which are directly associated with the system: 1) a bedrock electrical resistivity low, and 2) an area of relatively high near-surface temperatures.

The magnetic low occurs at the intersection of two major structural zones which are defined by magnetic lineations, mapped faults, and topographic features which coincide with a complementary set of strike-slip fault zones determined from seismic activity (Weaver and Walter, 1977). The intersection of these two zones of active tectonism probably served as the locus for emplacement of a pluton at depth, above which are observed the coincidental geophysical anomalies and surface manifestations related to the geothermal system.

ACKNOWLEDGEMENTS

This work was funded by Department of Energy, Division of Geothermal Energy contract EY-76-S-07-1601. Related Coso studies are being continued under Department of Energy, Division of Geothermal Energy contract EG-78-C-07-1701. The author thanks Charles R. Bacon and William F. Isherwood of the United States Geological Survey for their review of and comments on this report.

REFERENCES

Combs, J., 1975, Heat flow and microearthquake studies, Coso geothermal area, China Lake, California: Final Report, Contract No. NOO 123-74-2099, Program code 4F10, sponsored by ARPA.

Duffield, W. A., and Bacon, C. R., 1977, Preliminary geologic map of the Coso volcanic field and adjacent areas, Inyo County, California: US Geol. Sur. Open File Map 77-311, 2 sheets.

Fox, R. C., 1978, Dipole-dipole resistivity survey of a portion of the Coso Hot Springs KGRA, Inyo County, California: UURI-ESL Report, DOE Contract EY-76-S-07-1601.

Furgerson, R. B., 1975, Progress report on electrical resistivity studies Coso Geothermal Area, Inyo County, California: Naval Weapons Center Tech. Pub. S497., China Lake, Calif.

Hulen, J. B., 1978, Geology and alteration of the Coso Hot Springs Geothermal Area, Inyo County, California: UURI-ESL Report, DOE Contract EG-78-C-07-1701.

Lanphere, M. A. and Dalrymple, G. B., 1975, K-Ar ages of Pleistocene rhyolitic volcanism in the Coso Range, California: Geology, V. III, pp. 339-341.

LeSchack, L. A., Lewis, J. E., and Chang, D. C., 1977, Rapid reconnaissance of geothermal prospects using shallow temperature surveys: Semi-annual technical report (December). Development and Resources Transportation Co., DOE Contract EG-77-C-01-4021.

USGS, 1976, Residual Magnetic Intensity Map, Coso Hot Springs, California: Open File Report 76-698.

Weaver, C. S. and Walter, A. W., 1977, Strike-slip fault zones and crustal spreading in the Coso Range, California: USGS Preliminary Report (in preparation).

DISTRIBUTION LIST

External

David N. Anderson	Geothermal Resources Council, Davis, CA.
R.J. Andrews	Rocky Mountain Well Log Services, Denver, CO.
James K. Applegate	Boise State University, Boise, ID.
Sam Arentz, Jr.	Steam Corporation of America, Salt Lake City, UT.
Carl F. Austin	Geothermal Technology, NWC, China Lake, CA.
Lawrence Axtell	Geothermal Services, Inc., San Diego, CA.
Charles Bacon	USGS, Menlo Park, CA.
C. Forest Bacon	California Division of Mines & Geology, Sacramento, CA.
Larry Ball	DOE/DGE, Washington, DC.
Ronald Barr	Earth Power Corporation, Tulsa, OK.
H.C. Bemis	Fluid Energy Corporation, Denver, CO.
David D. Blackwell	Southern Methodist University, Dallas, TX.
Gunnar Bodvarsson	Oregon State University, Corvallis, OR.
C.M. Bonar	Atlantic Richfield Co., Dallas, TX.
David Boore	Stanford University, Stanford, CA.
Roger L. Bowers	Hunt Energy Corporation, Dallas, TX.
Jim Bresee	DOE/DGE, Washington, DC.
A.J. Brinker	Al-Aquitaine Exploration, Ltd., Denver, CO.
William D. Brumbaugh	Conoco, Ponca City, OK.
Larry Burdge	EG&G Idaho, Idaho Falls, ID.
Scott W. Butters	Terra Tek, Salt Lake City, UT.
Glen Campbell	Gulf Min. Resource Company, Denver, CO.
Bob Christiansen	USGS, Menlo Park, CA.
Eugene V. Ciancanelli	Consulting Geologist, San Diego, CA.
Jim Combs	Geothermal Services, Inc., San Diego, CA.
F. Dale Corman	O'Brien Resources, Inc., Kentfield, CA.
Ritchie Coryell	National Science Foundation, Washington, DC.
R. Corwin	University of California, Berkeley, CA.
James Cotter	DOE/NV, Las Vegas, NV.
Gary Crosby	Phillips Petroleum Company, Del Mar, CA.
K.R. Davis	Thermal Power Company, San Francisco, CA.
Jere Denton	Southland Royalty Company, Fort Worth, TX.
William Dolan	Amax Exploration Inc., Denver, CO.
Earth Sciences Division Library	Lawrence Berkeley Laboratory, Berkeley, CA.
Robert C. Edmiston	Chevron Resources Company, San Francisco, CA.
Wilf Elders	University of California, Riverside, CA.
Samuel M. Eisenstat	Geothermal Exploration Company, New York, NY.
M.C. Erskine, Jr.	Eureka Resource Associates, Berkeley, CA.
Domenic J. Falcone	Geothermal Resources International, Marina del Rey, CA.
Glen Faulkner	USGS, Water Resources Division, Menlo Park, CA.
Val A. Finlayson	Utah Power and Light Company, Salt Lake City, UT.
Joseph N. Fiore	DOE/NV, Las Vegas, NV.
Robert T. Forest	Phillips Petroleum Company, Reno, NV.

Robert O. Fournier	USGS, Menlo Park, CA.
Frank Frischknecht	U.S. Geological Survey, Denver, CO.
Gary Galyardt	U.S. Geological Survey, Denver, CO.
N.E. Goldstein	Lawrence Berkeley Laboratory, Berkeley, CA.
Steven M. Goldstein	The Mitre Corporation, McLean, VA.
Bob Greider	Intercontinental Energy Co., Denver, CO.
John Griffith	DOE/ID, Idaho Falls, ID.
J.H. Hafenbrack	Exxon Co. USA, Denver, CO.
W.R. Hahman	Arizona Bureau of Geology & Mineral Technology Tucson, AZ.
Dee C. Hansen	Utah State Engineer, Salt Lake City, UT.
V. Nobel Harbinson	O'Brien Resources, Incorporated, Toronto, Ontario, Canada.
Norman Harthill	Group Seven, Incorporated, Golden, CO.
Margaret E. Hinkle	USGS-Exploration Research, Golden, CO.
John V. Howard	Lawrence Berkeley Laboratory, Berkeley, CA.
Don Hull	Oregon Dept. of Geology & Mineral Industries, Portland, OR.
Gerald W. Huttrer	Intercontinental Energy Corporation, Englewood, CO.
William F. Isherwood	USGS, Menlo Park, CA.
Dallas Jackson	USGS, Hilo, HI.
Jimmy J. Jacobson	Battelle Pacific Northwest Labs., Richland, WA.
Laurence P. James	Denver, CO.
George R. Jiracek	University of New Mexico, Albuquerque, NM.
Richard L. Jodry	Richardson, TX
Max Jones	Sierra Pacific Power, Reno, NV.
Lewis J. Katz	Utah Geophysical, Incorporated, Salt Lake City, UT.
Paul Kasameyer	Lawrence Livermore Laboratory, Livermore, CA.
George Keller	Colorado School of Mines, Golden, CO.
Paul Kintzinger	Los Alamos Scientific Laboratory, Jemez Springs, NM.
John W. Knox	Sunoco Energy Development Company, Dallas, TX.
James B. Koenig	Geothermex, Berkeley, CA.
Robert P. Koeppen	Oregon Institute Technology, Klamath Falls, OR.
Frank C. Kresse	Harding-Lawson Associates, San Rafael, CA.
Mark Landisman	University of Texas, Dallas, Richardson, TX.
Art Lange	AMAX Exploration, Incorporated, Denver, CO.
A.W. Laughlin	Los Alamos Scientific Laboratory, Los Alamos, NM.
Guy W. Leach	Oil Development Company of Texas, Amarillo,TX.
R.C. Lenzer	Phillips Petroleum Company, Del Mar, CA.
Paul Lienau	OIT, Klamath Falls, OR.
Mark A. Liggett	Cyprus Georesearch Company, Los Angeles, CA.
James O. McClellan	Geothermal Electric Systems Corporation, Salt Lake City, UT.
Robert B. McEuen	Woodward Clyde Consultants, San Francisco, CA.
Don C. McMillan	Utah Geological & Mineral Survey, Salt Lake City, UT.

J.R. McNitt	Energy and Mineral Development Branch, United Nations, NY.
Don R. Mabey	USGS, Denver, CO.
Skip Matlick	Republic Geothermal, Santa Fe Springs, CA.
Tsvi Meidav	Consultant, Berkeley, CA.
Frank G. Metcalfe	Geothermal Power Corporation, Novato, CA.
John Mitchell	Idaho Dept. of Water Resources, Boise, ID.
Frank Morrison	University of California, Berkeley, CA.
L.J. Patrick Muffler	USGS, Menlo Park, CA.
Clayton Nichols	DOE/DGE, Washington, DC.
H.E. Nissen	Aminoil USA, Houston, TX.
Denis Norton	University of Arizona, Tucson, AZ.
Franklin Olmsted	USGS, Menlo Park, CA.
Carel Otte	Union Oil Company, Los Angeles, CA.
Richard H. Pearl	Colorado Geological Survey, Denver, CO.
Wayne Peeples	Southern Methodist University, Dallas, TX.
B.J. Perry	Mono Power Company, Rosemead, CA.
Harvey S. Price	Intercomp Resource Development & Engineering Inc. Houston, TX.
Alan O. Ramo	Sunoco Energy Development Company, Dallas, TX.
Robert W. Rex	Republic Geothermal, Inc., Santa Fe Springs, CA.
Barbara Ritzma	Science & Engineering Department, University of Utah, Salt Lake City, UT.
Jack Salisbury	DOE/DGE, Washington, DC.
Robert San Martin	New Mexico Energy Institute, Las Cruces, NM.
Konosuke Sato	Metal Mining Agency of Japan, Minato-Ku, Tokyo.
Robert Schultz	EG&G Idaho, Idaho Falls, ID.
John V.A. Sharp	Hydrosearch, Inc., Reno, NV.
Wayne Shaw	Getty Oil Company, Bakersfield, CA.
Gregory L. Simay	City of Burbank, Public Service Dept., Burbank, CA.
W.P. Sims	DeGolyer and MacNaughton, Dallas, TX.
H.W. Smith	University of Texas, Austin, TX.
John Sonderegger	Montana Bureau of Mines & Geology, Butte, MT.
Neil Stefanides	Union Oil Company, Los Angeles, CA.
R.C. Stoker	EG&G Idaho, Idaho Falls, ID.
Reid Stone	USGS, Menlo Park, CA.
Paul V. Storm	California Energy Company, Santa Rosa, CA.
W.K. Summers	W.K. Summers & Associates, Socorro, NM.
Chandler Swanberg	New Mexico State University, Las Cruces, NM.
Charles M. Swift, Jr.	Chevron Oil Company, San Francisco, CA.
J.B. Syptak	Anadarko Production Company, Houston, TX.
Robert L. Tabbert	Atlantic Richfield Company, Dallas, TX.
Bernard Tillement	Aquitaine Company of Canada, Calgary, Canada.
Ronald Toms	DOE/DGE, Washington, DC.
Dennis T. Trexler	Nevada Bureau of Mines & Geology, Reno, NV.
John Tsiaperas	Shell Oil Company, Houston, TX.
Jack Von Hoene	Davon, Inc., Milford, UT.
John Walker	DOE/DGE, Washington, DC.
D. Roger Wall	Aminoil USA, Inc., Santa Rosa, CA.

Paul Walton	American Geological Enterprises, Inc., Salt Lake City, UT.
Maggie Widmayer	DOE/ID, Idaho Falls, ID.
Syd Willard	California Energy Commission, Sacramento, CA.
David Williams	DOE/DGE, Washington, DC.
Paul Witherspoon	Lawrence Berkeley Laboratory, Berkeley, CA.
Harold Wollenberg	Lawrence Berkeley Laboratory, Berkeley, CA.
William B. Wray, Jr.	VanCott, Bagley, Cornwall & McCarthy, Salt Lake City, UT.
B.J. Wynat	Occidental Geothermal, Inc., Bakersfield, CA.
Paul C. Yuen	University of Hawaii @ Manoa, Honolulu, HI.
S.H. Yungul	Chevron Resources Company, San Francisco, CA.
Eliot J. Zais	Elliot Zais & Associates, Corvallis, OR.

Internal

W. Ursenbach	UURI, Salt Lake City, UT.
S.H. Ward (2)	UU/GG, Salt Lake City, UT.
J.A. Whelan	UU/GG, Salt Lake City, UT.
P.M. Wright	ESL/UURI, Salt Lake City, UT.
H.P. Ross	ESL/UURI, Salt Lake City, UT.
R.C. Fox	ESL/UURI, Salt Lake City, UT.
Master Report File	ESL/UURI, Salt Lake City, UT.

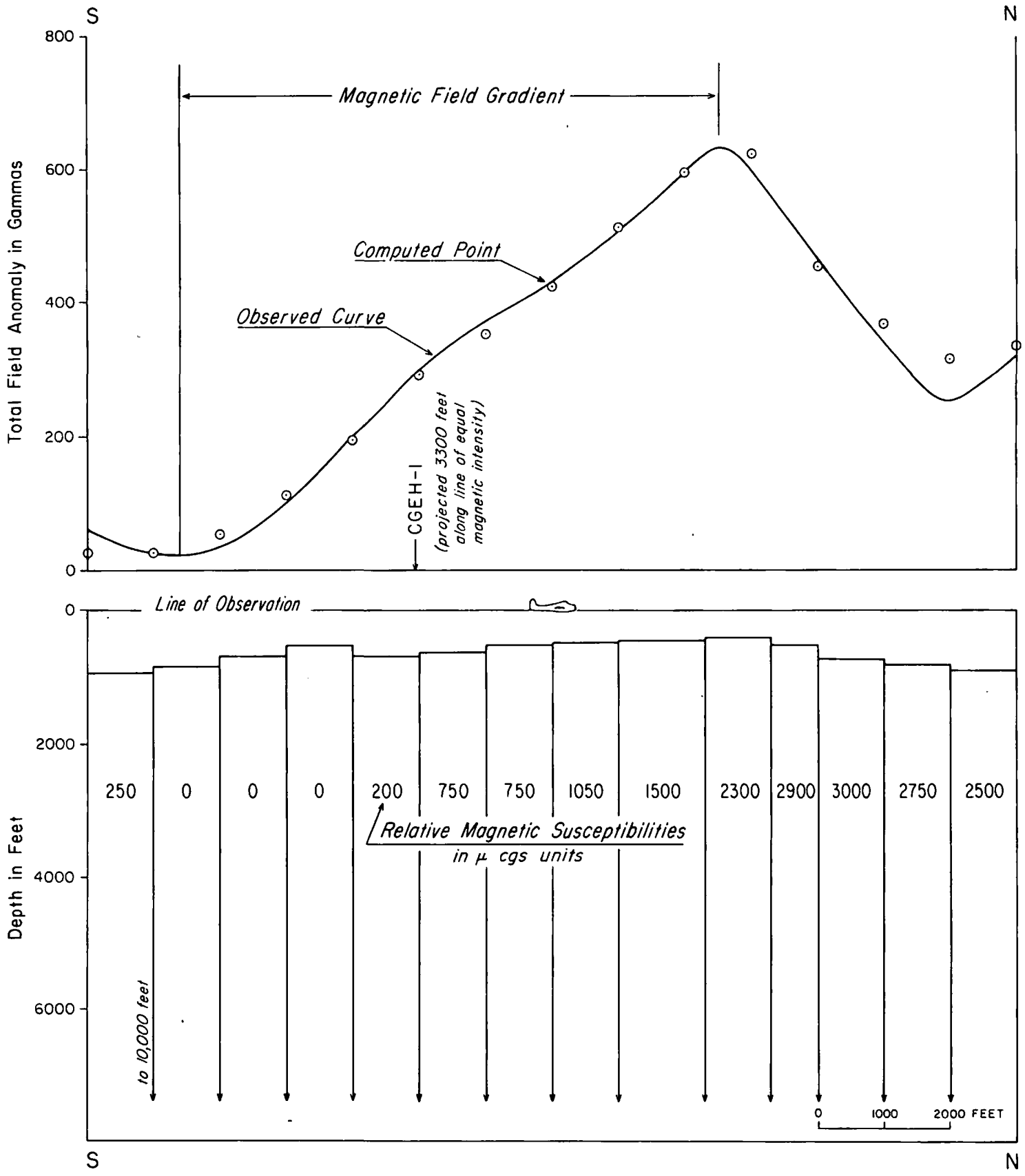

FIGURE 3

ANALYSIS OF MAGNETIC FIELD GRADIENT

(see Plate 3 for location of profile)

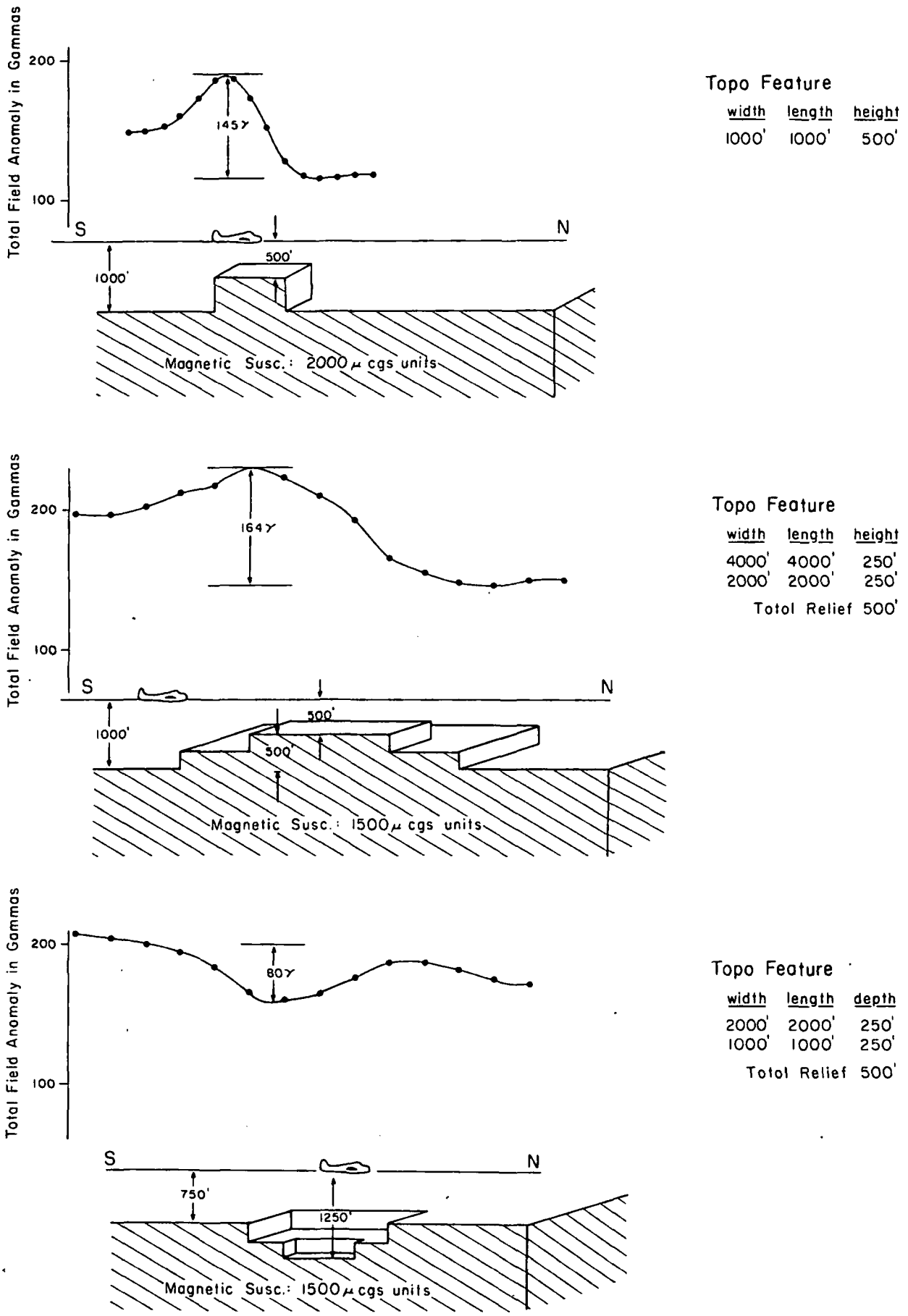

FIGURE 2

TOPOGRAPHIC EFFECT MAGNETIC ANOMALIES

Earth's Magnetic Field Strength: 50,000 gammas

Declination = 16° E; Inclination = 60°


CALIFORNIA
0 20 40 60 80
MILES
N
LOCATION MAP
COSO HOT SPRINGS
KGRA
OREGON
DEL NORTE
Crescent City
Yreka
MODOC
Alturas
SISKIYOU
HUMBOLDT
Eureka
TRINITY
Weaverville
SHASTA
Redding
LASSEN
Susanville
Red Bluff
TEHAMA
PLUMAS
Quincy
MENDOCINO
GLENN
Willows
BUTTE
Oroville
SIERRA
Downieville
COLUSA
NEVADA
Ukiah
Lake-port
Colusa
Yuba City
YUBA
Marysville
Nevada City
LAKE
PLACER
Auburn
YOLO
SUTTER
EL DORADO
Placerville
SONOMA
NAPA
Wood land
Sacramento
Markleeville
Santa Rosa
Napa
Fair-field
SACRA-MENTO
AMADOR
Jackson
ALPINE
CALAVERAS
Bridgeport
MARIN
SOLANO
SAN JOAQUIN
San Andreas
TUOLUMNE
San Rafael
Martinez
CONTRA COSTA
Stockton
Sonora
San Francisco
SAN FRANCISCO
Oakland
ALAMEDA
Modesto
MARIPOSA
Mariposa
MONO
Redwood City
SAN MATEO
San Jose
STANISLAUS
SANTA CLARA
Merced
MADERA
SANTA CRUZ
Santa Cruz
MERCED
Madera
FRESNO
Hollister
Salinas
SAN BENITO
Fresno
Independence
Hanford
Visalia
INYO
MONTEREY
KINGS
TULARE
SAN LUIS OBISPO
Bakersfield
San Luis Obispo
KERN
SAN BERNADINO
SANTA BARBARA
VENTURA
LOS ANGELES
Santa Barbara
Ventura
Los Angeles
San Bernardino
Riverside
Santa Ana
RIVERSIDE
ORANGE
ARIZ.
SAN DIEGO
IMPERIAL
San Diego
El Centro
MEXICO

FIGURE 1

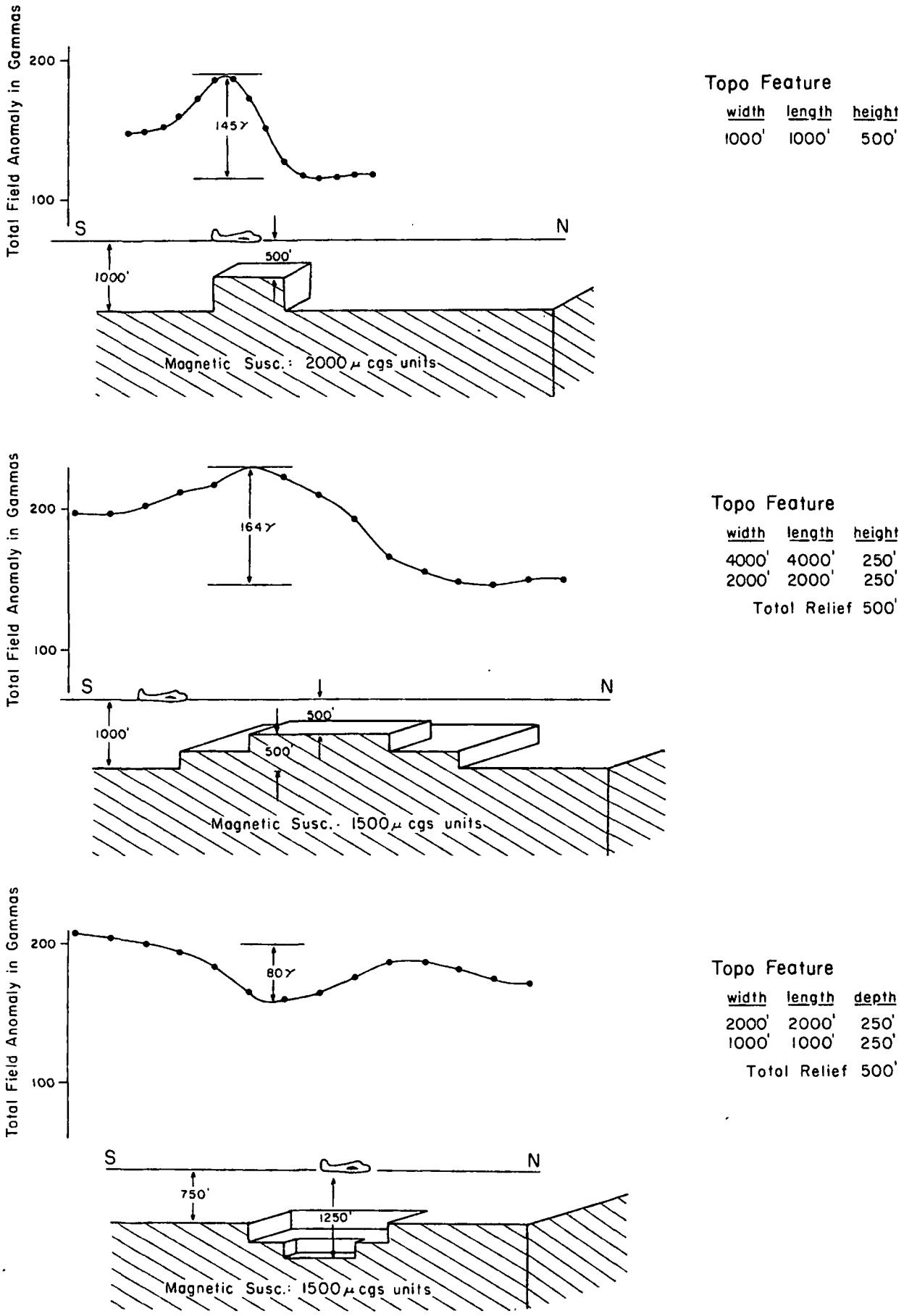

FIGURE 2

TOPOGRAPHIC EFFECT MAGNETIC ANOMALIES

Earth's Magnetic Field Strength: 50,000 gammas

Declination = 16°E; Inclination = 60°

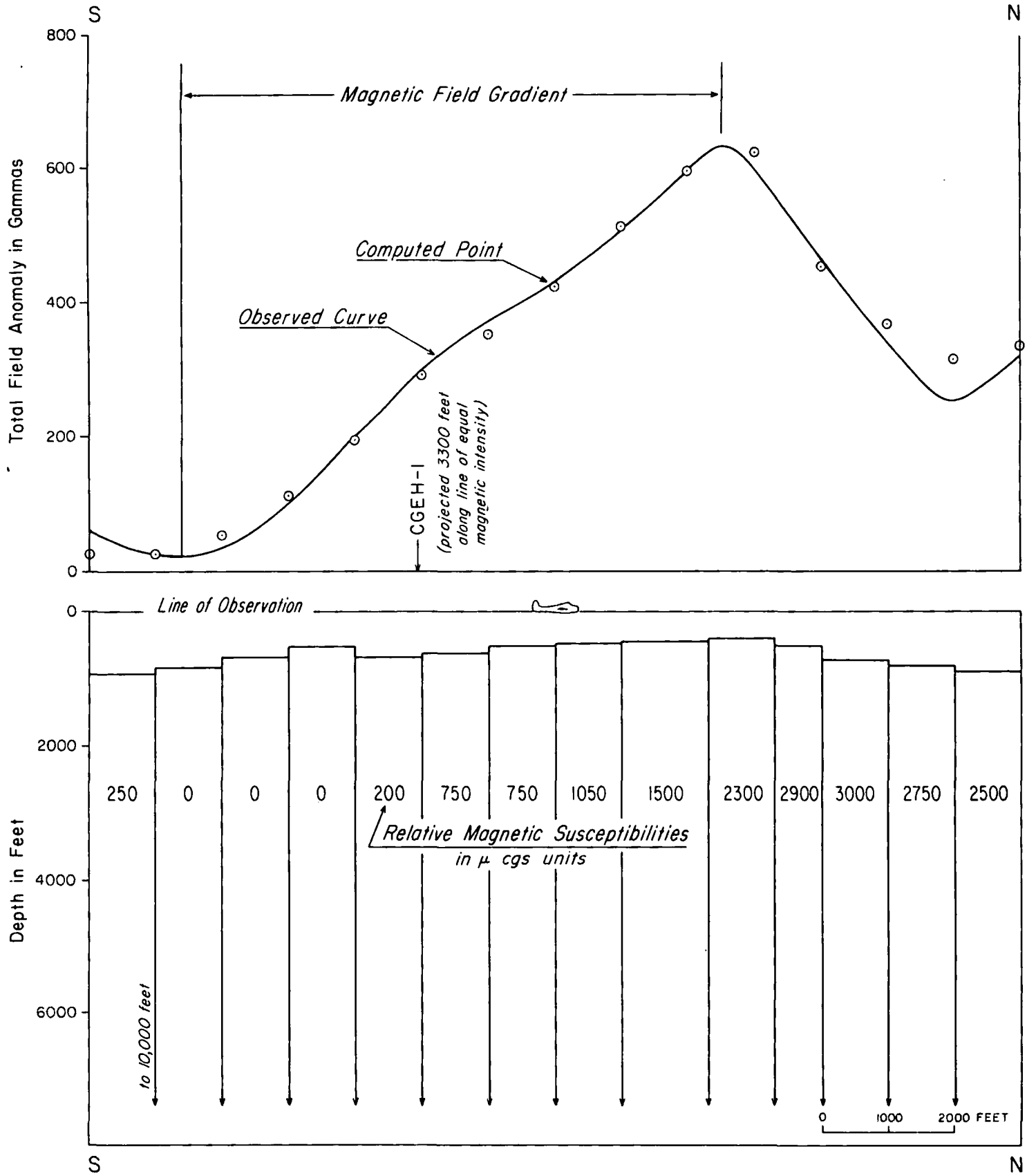

FIGURE 3

ANALYSIS OF MAGNETIC FIELD GRADIENT

(see Plate 3 for location of profile)